Journal of Orthopaedics 16 (2019) 206–210

Contents lists available at ScienceDirect

Journal of Orthopaedics

journal homepage: www.elsevier.com/locate/jor

Short tau inversion recovery magnetic resonance imaging for staging and screening in myxoid liposarcoma

Alexander Chien[a], Craig W. Zuppan[b], Li Lei[d], Nadine L. Williams[c], Troy G. Shields[c], Joseph G. Elsissy[c], Peter Pham[a], Lee M. Zuckerman[c,*]

[a] Department of Radiology, Loma Linda University Medical Center, 11234 Anderson Street, Loma Linda, CA, 92354, USA
[b] Department of Pathology, Loma Linda University School of Medicine, 11234 Anderson Street, Loma Linda, CA, 92354, USA
[c] Department of Orthopaedic Surgery, Loma Linda University Medical Center, 11406 Loma Linda Drive, Suite 218, Loma Linda, CA, 92354, USA
[d] Department of Pathology, Stanford University School of Medicine, 300 Pasteur Drive, Lane 235, Stanford, CA 94305-5324, USA

ARTICLE INFO

Keywords:
Myxoid liposarcoma
Magnetic resonance imaging (MRI)
Screening
Skeletal metastases

ABSTRACT

Purpose: Myxoid liposarcoma has a propensity to metastasize to bone. MRI is the preferred modality for detecting bone disease. We evaluated multiple MRI sequences to determine an optimal screening method.
Methods: Whole body MRI was performed on all patients. The number and locations of metastases found by imaging and round cell component of the sites sampled were evaluated.
Results: We found a total of 68 osseous lesions. Whole body MRI utilizing STIR only sequences decreased imaging time by 83.6% and demonstrated the lesions the best.
Conclusions: STIR sequences can be exclusively used during staging and screening of myxoid liposarcoma.

1. Introduction

Liposarcoma is the second most common soft tissue sarcoma with five distinct histologic subtypes.[1] The myxoid/round cell subtype comprises of approximately one third of the cases and is considered an intermediate grade sarcoma.[2] Myxoid liposarcoma (MLS) with a greater than 5% round cell component has been associated with a poorer prognosis.[3] Unlike other soft tissue sarcomas, a somewhat unusual feature of MLS is a propensity to metastasize to extrapulmonary sites such as the retroperitoneum, mediastinum, and bone.[2,4–6] Osseous metastasis have been reported to comprise from 4 to 58% of the metastatic events.[5–9] The osseous locations have been previously described to be within the spine, skull base, thoracic cage, pelvis, and upper and lower limbs.[8,9] There are numerous case reports and series that suggest that radiography, bone scintigraphy, and fluorodeoxyglucose positron emission tomography (FDG-PET) are relatively insensitive to metastatic bone disease in MLS, and that magnetic resonance imaging (MRI) may be the modality of choice for investigation.[5,8–12] However, MRI of the whole body utilizing multiple sequences is a time consuming endeavor utilizing significant resources, and thus is practically difficult to provide. Whole body MRI (WBMRI) examinations have also not been reimbursed by all insurers.

We cataloged the MRI characteristics and locations of the metastatic lesions, compared lesion detection of MRI to other imaging modalities, documented the round cell component of the primary tumor and metastatic deposits, and have subsequently modified our WBMRI protocol to more efficiently screen and stage our patients with MLS.

2. Materials and methods

2.1. Patients

After Institutional Review Board approval, a retrospective review yielded 9 patients with MLS in our institution between January 2012 and August 2018 whom underwent WBMRI evaluation. All patients had pathologic confirmation including FISH studies of the primary tumor and at least one metastatic focus if they developed metastatic disease. No patient had chemotherapy or radiation prior to sampling of the primary tumor or metastatic lesion. All patients had an R0 resection of the primary tumor and underwent adjuvant radiation to the site of resection.

2.2. Imaging protocol

Patients were staged with a WBMRI and CT of the chest, abdomen and pelvis. If a lesion was found on MRI in the bone marrow, a whole

* Corresponding author.
E-mail addresses: AChien@llu.edu (A. Chien), CZuppan@llu.edu (C.W. Zuppan), LiLei@Stanford.edu (L. Lei), NLWilliams@llu.edu (N.L. Williams), TShields@llu.edu (T.G. Shields), JElsissy@llu.edu (J.G. Elsissy), PPham@llu.edu (P. Pham), lzuckerman@llu.edu (L.M. Zuckerman).

https://doi.org/10.1016/j.jor.2019.02.023
Received 2 September 2018; Accepted 17 February 2019
Available online 28 February 2019
0972-978X/ Published by Elsevier, a division of RELX India, Pvt. Ltd on behalf of Prof. PK Surendran Memorial Education Foundation.

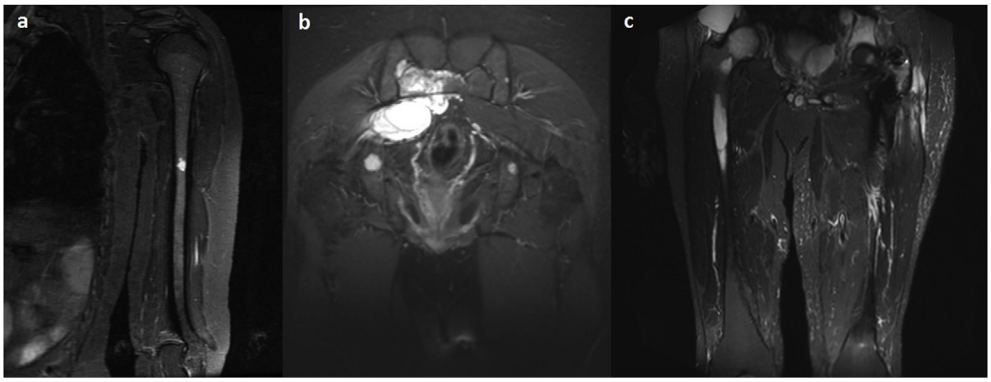

Fig. 1. Images depicting the wide view coronal images obtained with the STIR only protocol. (a) Images of the left humerus that include the chest with ribs and scapula. A metastatic lesion is noted in the humeral shaft. (b) Images of the pelvis demonstrating a sacral tumor with soft tissue extension and well as bilateral pubic rami tumors. (c) Images of both femurs after the patient's disease had progressed with diffuse osseous disease of the pelvis and femurs in addition to soft tissue metastases.

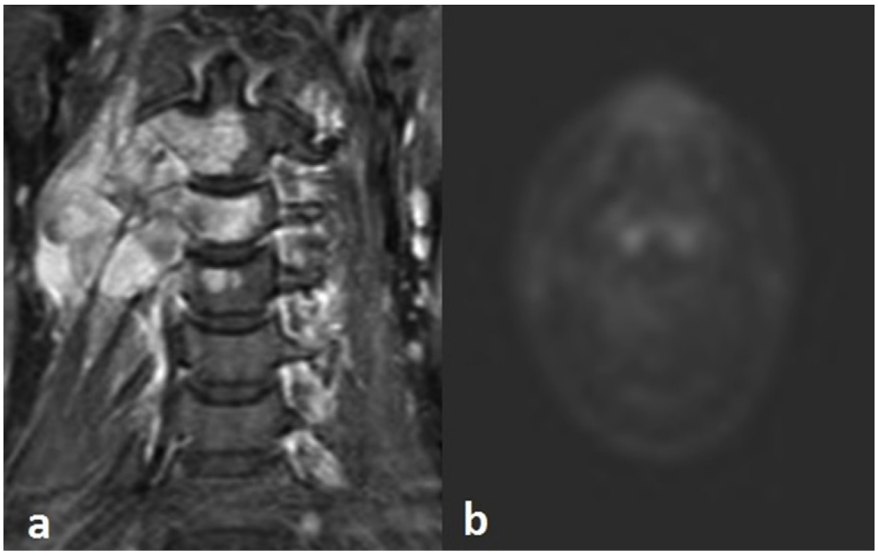

Fig. 2. Comparison of STIR MRI versus PET. (a) Coronal STIR MRI within the corresponding region of the (b) axial PET scan in the cervical spine demonstrating osseous and soft tissue metastases. The axial PET is negative.

body bone scan or PET-CT was also obtained for comparison. For the imaging performed at our institution, Siemens Symphony 1.5T and Siemens TrioTIM 3T MRI scanners were utilized. CT examinations were performed on a GE Lightspeed VCT, the bone scans were performed on a GE Optima NM/CT 640, and FDG-PET-CT were performed on a Siemens Biagraph MCT PET/CT.

The routine MRI evaluation for tumors and metastatic disease at our institution includes the following sequences: sagittal short tau inversion recovery (STIR), coronal STIR, axial STIR, axial T1, axial T1 fat suppressed, axial T1 fat suppressed post contrast, sagittal T1 fat suppressed post contrast, and coronal T1 fat suppressed post contrast. To accomplish WBMRI imaging, the protocol was applied to the cervical, thoracic, and lumbar spine, pelvis, and bilateral upper and lower extremities of each of these patients.

After initial staging was performed, patients were followed utilizing WBMRI with STIR only sequences. Large field coronal images were obtained of the bilateral chest to include the humerus, scapula and ribs, pelvis, and bilateral femurs (Fig. 1). Sagittal views of the cervical, thoracic and lumbar spine were obtained. Result interpretations were obtained from the original reads of the examinations and verified by the authors. Staging was performed every 3 months for the first 2 years after diagnosis, every 6 months between year 2 and year 5, and yearly afterwards.

3. Results

3.1. MRI findings

Three patients have not developed metastatic disease at 15, 18 and 48 months after initial diagnosis. Six patients were found to have metastatic disease. Two of the patients were found to have metastatic disease at the time of presentation. Four patients developed metastatic disease imaged by MRI at 14, 21, 36 and 54 months after initial diagnosis. A total of 68 separate metastatic bone lesions were found in our patients. All of the lesions were found on the STIR sequencing. The sites included the cervical spine (3 lesions), thoracic spine (9 lesions), lumbar spine (6 lesions), sacrum (11 lesions), ribs (4 lesions), humerus (4 lesions), scapula (1 lesion), iliac wing (8 lesions), acetabulum (7 lesions), superior pubic rami (2 lesions), inferior pubic rami (1 lesion) and femur (12 lesions). Of these tumors, soft tissue extension was noted in 8 of the lesions. Seven soft tissue only lesions were also found during screening. The locations included adjacent to the liver, upper arm, axilla, anterior thigh, posterior thigh, abdominal wall and ischiorectal fossa. No patients were found to have pulmonary metastases at any time during their follow-up.

3.2. Results of other imaging modalities

Other imaging modalities failed to demonstrate the bony lesions unless there was soft tissue extension of the tumor, except in one lesion found on bone scan in the femur and one in the iliac wing. Of the 8

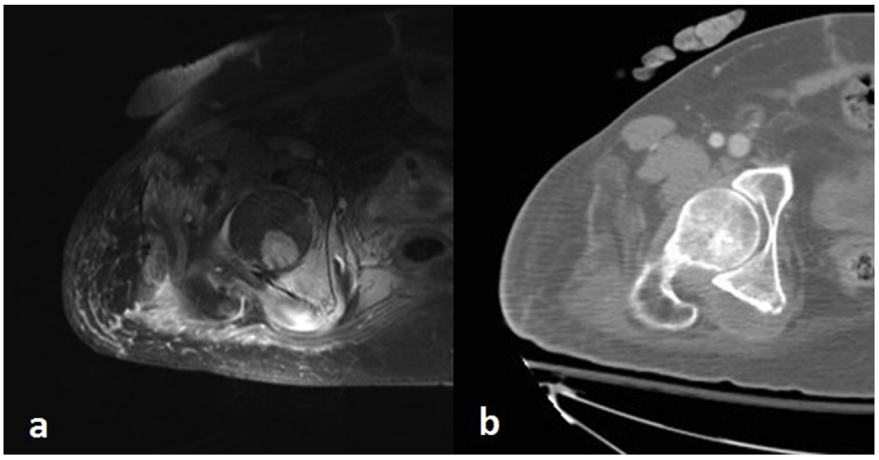

Fig. 3. Demonstration of metastatic disease found on both MRI and CT due to cortical breakthrough of the tumor. (a) Axial STIR MRI of the right hip demonstrating right femoral head, acetabular, and soft tissue lesions. (b) Corresponding axial bone window CT showing posterior acetabular cortical irregularity and soft tissue mass. Intraosseous lesions were not identified on CT.

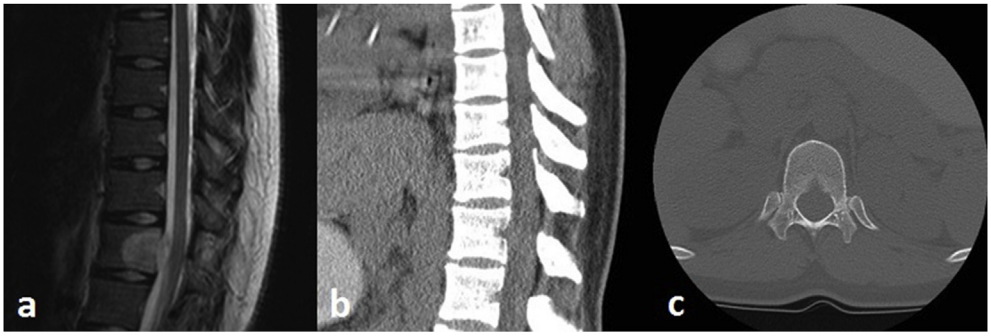

Fig. 4. Metastatic bone disease in the spine with cortical breakthrough not noted on CT. (a) Sagittal STIR MRI of T12 demonstrating a spinal metastasis extending into the spinal canal. (b) Corresponding sagittal soft tissue window CT and (c) axial bone window CT images of T12. The osseous portion and soft tissue portions were not seen on CT.

Fig. 5. Metastatic disease to the sacrum where only the soft tissue component was identified on CT and PET. (a) Axial STIR MRI demonstrating the left sacral lesion extending into the soft tissues anterior to sacrum, with an additional right iliac wing metastasis. (b) Corresponding soft tissue window CT demonstrating only the soft tissue component of the left sacral lesion. (c) Coronal STIR MRI demonstrating same left sacral lesion and soft tissue component with (d) PET scan demonstrating an FDG avid soft tissue component with equivocal osseous activity.

lesions with soft tissue extension, CT scan only found 4, and PET-CT only found 1 (Figs. 2 and 3). Of note, the CT missed 2 lesions in the thoracic spine where one had extension into the spinal canal (Fig. 4). The 1 lesion found on PET-CT did not demonstrate any uptake in the bony portion of the tumor while the soft tissue component had an SUV of 3.8 (Fig. 5).

3.3. Patient outcomes

Of the tumors resected in the patients with metastatic disease, 3 of the primary tumors had a round cell component of 0%, 1 of 2–5%, 1 of 5–10% and 1 of 20%. Ten of the metastatic lesions resected did not have any round cell component. Three patients with metastatic disease progressed on chemotherapy with multiple new tumors noted in the soft tissues and bone marrow. No pulmonary metastases were identified in these patients at any time during their follow-up. The patient diagnosed with metastatic disease at presentation progressed on chemotherapy and passed away 40 months after his initial diagnosis. The patient diagnosed with metastatic disease 21 months after diagnosis passed away 4 months later. The patients found to have metastatic disease at 20, 36 and 54 months after diagnosis are still alive at 80, 84 and 65 months after diagnosis, respectively.

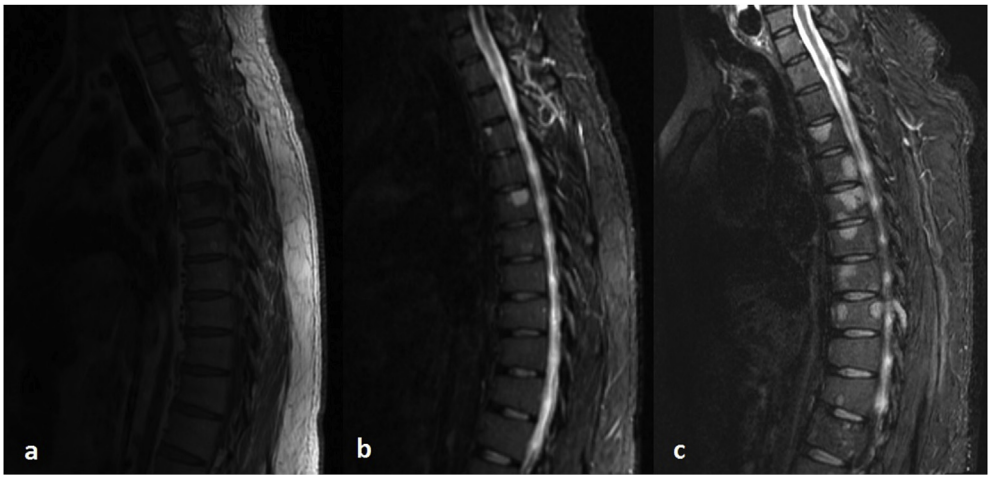

Fig. 6. Images depicting better visualization of metastases on STIR sequences when compared to T1 sequences. (a) T1 images of the thoracic spine with lesions at T2 and T4 that are not well visualized. (b) Corresponding STIR images with better visualization of the tumors. (c) Significant progression of disease with an increase in the size of the T2 and T4 lesions, in addition to multiple new tumors throughout the spine.

3.4. MRI features utilizing the STIR protocol

All of the metastases identified had MRI signal characteristics that were identical to the original soft tissue neoplasm, demonstrating low T1 weighted signal, and marked high signal on fluid sensitive sequences such as T2 fat suppressed and STIR sequences. The lesions also intensely enhanced post-contrast, either in a diffusely enhancing or heterogeneous enhancing pattern. All lesions were able to be identified on all MRI sequences. The lesions were most conspicuous using STIR and post contrast enhanced sequences due to the difference in contrast between the metastatic lesions and the normal bone marrow, cortical bone and soft tissue signal (Fig. 6).

These routine mass protocol MRI examinations averaged 250 min of total scan time for each patient. None of the patients could tolerate the entire exam in one session, and thus the examinations were divided up between 2 and 4 days. Subsequently, our STIR only protocol was performed after initial staging as a substitute for the routine mass protocol MRI of the whole body. The STIR WBMRI averaged 41 min of scan time, representing an 83.6% decrease in imaging time, and has been tolerated by all patients in one session.

4. Discussion

Metastatic lesions in patients with MLS are often found in extrapulmonary sites such as the osseous structures. Although the number of skeletal metastatic events from MLS are unclear, previous studies have shown osseous metastases to occur in 3%, 16%, 56%, 57% and 58% of patients.[2,6,8,9,12,13] In one series, 42% of the events occurred in the spine compared to 33% of 24 lesions found in the spine in a separate series.[8,9] The remaining 66% in this series were found in the pelvis (25%), thoracic cage (21%), upper limb (12%) and lower limb (8%).

Of our 6 patients with metastatic disease, 5 patients had osseous metastasis. Thirty-three of the 68 lesions involved the axial skeleton. Five of these lesions involved the upper extremity and 12 involved the lower extremity. No pulmonary metastases were identified. One patient developed 6 soft tissue only metastases located in the pelvis and extremities. Although the axial skeleton appears to be the most common site of disease, a substantial number involved the pelvis and extremities.

When evaluated on FDG-PET imaging, no osseous only lesions were identified. Only the soft tissue component of a sacral metastases was FDG avid. It has been theorized that PET may not demonstrate high activity in MLS because the myxoid stroma may prevent the labeled glucose from reaching the cells in sufficient quantity to be detected by the PET scanner.[7] In addition, many of the MRI identified osseous lesions were small in size, and potentially not large enough to identify within the resolution of PET. Therefore metastatic lesions may be occult on FDG-PET.

When evaluated by CT exam, no osseous only lesions were identified. Only lesions that broke through the cortex of the bone were discovered on CT. Still, two thoracic osseous lesions extending into the soft tissues could not be identified. This finding is concerning that disease that may impinge on the spinal cord may not be detectable on routine CT screening.

There were no FDG-PET, CT, or scintigraphic lesions identified that were not also visualized by MRI. Our findings support that WBMRI should be the preferred modality to screen for metastatic MLS. Although reports suggest that MLS with > 5% round cell component has a poorer prognosis, only 2 out of 3 patients with a round cell component > 5% developed metastatic disease.[3] Four of the 6 patients with a round cell component between 0 and 5% developed metastatic disease. Stevenson et al. found 2 out of 28 patients with metastatic disease at presentation.[8] Both of these patients had a 0% round cell component. The pathology of the metastatic lesions in the two patients with a low round cell component also demonstrated < 5% round cell component. Given that we had patients with < 5% round cell component demonstrate osseous metastatic disease, we do not utilize the percentage of round cell component as a reason not to do whole body screening for metastases.

By utilizing WBMRI as a method of disease screening and staging, our data suggests that osseous metastatic disease may be even more prevalent than previously thought, and could be the most common location. We found the MRI characteristics of metastatic MLS were identical to the original soft tissue neoplasm, demonstrating low T1 signal and bright STIR imaging characteristics. There was intense contrast enhancement with gadolinium, which is similar to previous reports in the literature.[1,14] Given the major time commitment necessary to perform WBMRI examinations with multiple sequences, our institution is now performing screening with STIR only images, such as utilized in patients with multiple myeloma.[15] This protocol includes sagittal sequences of the cervical, thoracic and lumbar spine. Coronal large field of view sequences are employed for the bilateral chest (including the humerus and ribs), pelvis and bilateral femurs. All the lesions in our series were able to be detected on these sequences. Performing a STIR screening protocol has decreased the MRI whole body imaging acquisition time to 41 min, with total MRI room time being approximately 80 min and a decrease in imaging time of 83.6%. This protocol is well tolerated by patients in a single visit and decreases the utilization time compared to obtaining multiple sequences. This protocol also avoids using contrast during this screening process.

A limitation of this protocol is that other findings may mimic metastatic disease. Our initial experience suggests that whole body STIR may be subject to false positive reports, as findings such as red marrow reconversion, vertebral body hemangiomas, osseous enchondromas, as

well as acetabular cysts from underlying hip labral pathology may mimic metastasis. Seo et al. also reported a nerve sheath tumor mimicking metastatic disease.[16] If a potential false positive lesion is seen on the screening examination, a dedicated contrast enhanced MRI is performed to further characterize the lesion. In general, we find that the lesions of MLS are "lightbulb" bright in their STIR characteristics, which potentially differentiates it from marrow conversion and vertebral body hemangiomas. Acetabular cysts can be suspected if they occur adjacent to the hip labrum, and nerve sheath tumors may be considered if the lesion lies along the course of a peripheral nerve. We do believe that some of the indeterminate lesions may need additional workup. At this time, we are continuing to assess the original tumor bed for local recurrence with our standard MRI post-operative tumor protocol as scarring and radiation changes may affect the STIR sequences.

Although this retrospective study only included 9 patients, a total of 68 bony lesions were demonstrated. A limitation of this number is that even though all of our suspected metastatic lesions were identical in MRI characteristics with "fluid bright" STIR signal and enhancement, only 10 of our MRI identified metastatic lesions were biopsy proven. All six of these patients have undergone follow up imaging demonstrating an increase in size of the suspected lesions as well as the development of new lesions. Given the small size of our study, sensitivity and specificity could not be assessed. However, we noted that MRI identified far more lesions with imaging features of metastatic tumor in our 6 patients than FDG-PET, CT or scintigraphic imaging, and therefore appears to be a better imaging modality for this purpose.

5. Conclusions

Metastatic MLS is most reliably detected on WBMRI. We found that imaging the whole body with standard mass evaluation MRI to be a resource consuming endeavor. Given that the signal characteristics of metastatic MLS are quite conspicuous on STIR and gadolinium enhanced post contrast sequences, our institution has begun to screen these patients with STIR sequences of the whole body. Whole body STIR has markedly decreased imaging time, which is better tolerated by our patients and decreases the utilization time of the MRI. This has also avoided complications that may occur with administering contrast.

Although a round cell component of < 5% is felt to be a good prognostic factor, we found patients that demonstrated metastatic events in tumors with a 0% round cell component. Due to this, we advocate that all patients diagnosed with MLS obtain a WBMRI with STIR sequences for both staging and screening.

Conflicts of interest

No benefits in any form have been or will be received from a commercial party related directly or indirectly to the subject of this manuscript.

Funding

This research did not receive any specific grant from funding agencies in the public, commercial, or not-for-profit sectors.

Appendix A. Supplementary data

Supplementary data to this article can be found online at https://doi.org/10.1016/j.jor.2019.02.023.

References

1. Murphey MD, Arcara LK, Fanburg-Smith J. From the archives of the AFIP: imaging of musculoskeletal liposarcoma with radiologic-pathologic correlation. *Radiographics.* 2005;25:1371–1395.
2. Noble JL, Moskovic E, Fisher C, Judson I. Imaging of skeletal metastases in myxoid liposarcoma. *Sarcoma.* 2010;2010:262361.
3. Antonescu CR, Tschernyavsky SJ, Decuseara R, et al. Prognostic impact of P53 status, TLS-CHOP fusion transcript structure, and histological grade in myxoid liposarcoma: a molecular and clinicopathologic study of 82 cases. *Clin Cancer Res.* 2001;7:3977–3987.
4. Schwab JH, Healey JH. FDG-PET lacks sufficient sensitivity to detect myxoid liposarcoma spinal metastases detected by MRI. *Sarcoma.* 2007;2007:36785.
5. Ishii T, Ueda T, Myoui A, Tamai N, Hosono N, Yoshikawa H. Unusual skeletal metastases from myxoid liposarcoma only detectable by MR imaging. *Eur Radiol.* 2003;13(Suppl 4):L185–L191.
6. Schwab JH, Boland P, Guo T, et al. Skeletal metastases in myxoid liposarcoma: an unusual pattern of distant spread. *Ann Surg Oncol.* 2007;14:1507–1514.
7. Sakamoto A, Fukutoku Y, Matsumoto Y, Harimaya K, Oda Y, Iwamoto Y. Myxoid liposarcoma with negative features on bone scan and [18F]-2-fluoro-2-deoxy-D-glucose-positron emission tomography. *World J Surg Oncol.* 2012;10:214.
8. Stevenson JD, Watson JJ, Cool P, et al. Whole-body magnetic resonance imaging in myxoid liposarcoma: a useful adjunct for the detection of extra-pulmonary metastatic disease. *Eur J Surg Oncol.* 2016;42:574–580.
9. Sheah K, Ouellette HA, Torriani M, Nielsen GP, Kattapuram S, Bredella MA. Metastatic myxoid liposarcomas: imaging and histopathologic findings. *Skeletal Radiol.* 2008;37:251–258.
10. Hanna SA, Qureshi YA, Bayliss L, et al. Late widespread skeletal metastases from myxoid liposarcoma detected by MRI only. *World J Surg Oncol.* 2008;6:62.
11. Conill C, Setoain X, Colomo L, et al. Diagnostic efficacy of bone scintigraphy, magnetic resonance imaging, and positron emission tomography in bone metastases of myxoid liposarcoma. *J Magn Reson Imag.* 2008;27:625–628.
12. Schwab JH, Boland PJ, Antonescu C, Bilsky MH, Healey JH. Spinal metastases from myxoid liposarcoma warrant screening with magnetic resonance imaging. *Cancer.* 2007;110:1815–1822.
13. Tateishi U, Hasegawa T, Beppu Y, Kawai A, Satake M, Moriyama N. Prognostic significance of MRI findings in patients with myxoid-round cell liposarcoma. *AJR Am J Roentgenol.* 2004;182:725–731.
14. Sung MS, Kang HS, Suh JS, et al. Myxoid liposarcoma: appearance at MR imaging with histologic correlation. *Radiographics.* 2000;20:1007–1019.
15. Hanrahan CJ, Christensen CR, Crim JR. Current concepts in the evaluation of multiple myeloma with MR imaging and FDG PET/CT. *Radiographics.* 2010;30:127–142.
16. Seo SW, Kwon JW, Jang SW, Jang SP, Park YS. Feasibility of whole-body MRI for detecting metastatic myxoid liposarcoma: a case series. *Orthopedics.* 2011;34:e748–e754.